Journal of Electronics and Advanced Electrical Engineering
Volume 1 | Issue 1

HELICS GROUP
Scientific Networks

Research Article Open Access

Method of Far-field Electromagnetic Radiation Prediction and Suppression Based on Equivalence of Capacitance Parameters in Power Converter System

Li Zhengzhi[1*], Zhang Kaiyan[1], Wang Shishan[1] and A Guo Jian[1]

[1]College of Automation and Engineering, Nanjing University of Aeronautics and Astronautics, Nanjing, Jiangsu, China

Corresponding author: *Li Zhengzhi, College of Automation and Engineering, Nanjing University of Aeronautics and Astronautics, Nanjing, Jiangsu, China, E-mail: Lzz147258369@qq.com*

Citation: Zhengzhi L, Kaiyan Z, Shishan W, Jian G (2020) Method of Far-field Electromagnetic Radiation Prediction and Suppression Based on Equivalence of capacitance parameters in Power Converter System, J Electron Adv Electr Eng 1(1): 22-27.
https://doi.org/10.47890/JEAEE/2020/LZhengzhi/11120005

Received Date: April 01, 2020; **Accepted Date:** April 20, 2020; **Published Date:** April 29, 2020

Abstract

Electromagnetic radiation is one of the key issues in research area of EMC. This paper analyzes that common-mode (CM) current is the main noise source, and transmits through parasitic capacitances between input cables and ground, thus CM current path model (CCP) is established. Moreover, CCP is formed as equivalent prediction model of radiation (EMR) by appropriate simplification. The parasitic capacitances of EMR are extracted, and EMR is iterative designed. Furthermore, the radiation emission of two models is in good agreement. At last, ferrite magnetic ring is selected to change scattering parameter matrix, thus electromagnetic radiation can be suppressed; the recommended installation of magnetic ring is given.

Index Terms: Radiation; Parasitic Parameter;

Introduction

The trend of high frequency and high-power density of power converter is more and more obvious, and the electromagnetic interference (EMI) produced by power converter is more and more serious. As an important index of power converter EMI, far-field electromagnetic radiation emission is not only easy to affect the normal operation of nearby wireless electronic equipment, but also often causes the electromagnetic radiation emission of (30-300) MHz bands to exceed the standard, which fails to pass the EMC certification of power converter and the electrical and electronic systems powered by it. Meanwhile, the EMC certification becomes a difficulty and challenge in the design of power converter [1,2].

Due to the complexity of the structure of power converter, the research on the emission mechanism and characteristics of far-field electromagnetic radiation of power converter at home and abroad is less than that of conducted interference [3,4], and it is difficult to establish accurate and simplified radiation prediction model, so it is very urgent to model the power converter system reasonably and effectively [5-8].

The prediction of electromagnetic noise is aimed to suppress it, so that all kinds of products would pass the corresponding standard limits. There are many suppression schemes of radiation noise such as EMI filter can be added or PCB structure can be adjusted, but the cost is high and the economy is bad. Ferrite magnetic ring is the main way to suppress radiation noise. However, there are few literatures on the suppression of radiation interference by ferrite magnetic ring and the mechanism analysis is not clear [9,10]. Similar literatures such as [11] only study the change of cable induced current after magnetic ring is installed. While literature [12,13] only conduct qualitative analysis and repetitive test research without quantifying the suppression effect.

Based on the principle of capacitance equivalence, through the numerical calculation method, this paper explores an equivalent radiation prediction model which can represent the radiation characteristics, and estimates the radiation field strength in the way of experiment; at the same time, it also analyzes the mechanism of suppressing radiation noise by using the scattering parameters in detail, so that the suppression effect can be evaluated quickly, Therefore, it provides an effective and easy to implement prediction and suppression scheme for the electromagnetic radiation of power converter system.

Electromagnetic noise radiation model

Radiated noise source

There are two kinds of electromagnetic noise produced by power converter: differential mode (DM) noise and common mode (CM) noise (Figure 1). DM noise mainly flows through the working circuit of the converter, while CM noise propagates through the parasitic capacitance between the power line and the ground.

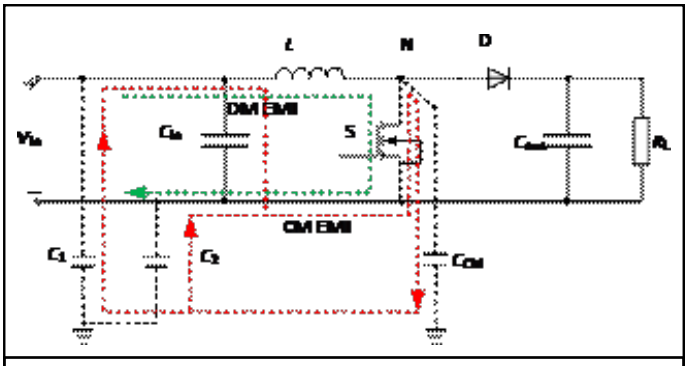

Figure1: CM and DM noise in boost converter

In the Boost converter, the length of input cable is the electrical size (λ > 1/10). When the Boost is working, there exist high-frequency voltage harmonics in the drain-source voltage V_{ds}, which drives the high-frequency current to flow through the working circuit composed of inductor L, input capacitor C_{in} and DC power supply, generating DM noise of the converter. Also, V_{ds} drives the high-frequency current to flow through the working circuit composed of C_{cm}, ground, C_1 and C_2(C_{cm} represents capacitor between the node N and ground; C_1 and C_2 represent parasitic capacitances between the cables and the ground). Given The electric fields generated by DM current cancel each other in the far field since the converter is electrically small, this paper mainly concerns far-field radiation caused by CM current (Figure 2).

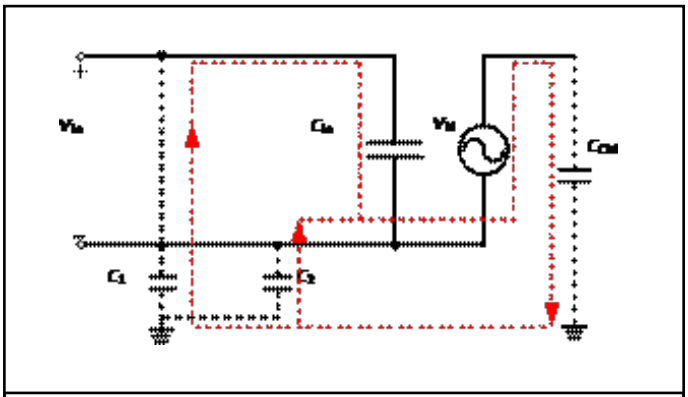

Figure 2: CM Path in Boost converter

When the converter is working, the high-frequency switching in MOSFET S causes voltage spike and current spike, which leads to high du/dt, generates a lot of electromagnetic noise and propagates to outside with the form of electromagnetic radiation. Therefore, V_N can substitute for S. In the frequency bands of radiation (30~300MHz), the impedance of C_{in} and C_{out} is very small compared with the impedance of parasitic capacitances C_{CM}, C_1 and C_2, which can be regarded as short circuit, while the impedance of inductance L is very large, which can be regarded as open circuit. Then, we can get the simplified CM path (Figure 3).

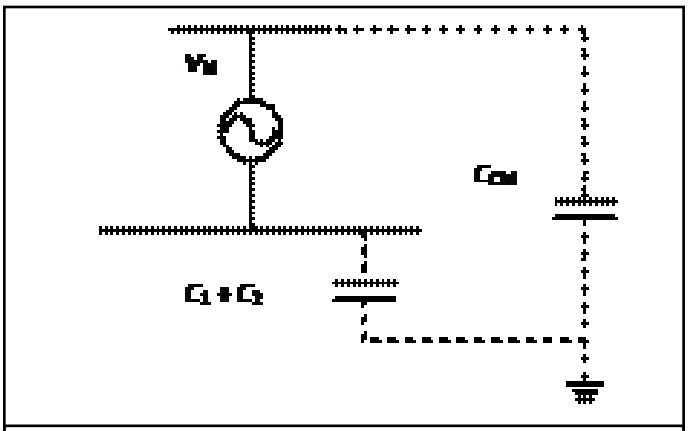

Figure 3: Simplified path of CM current

Equivalent Prediction Model of Radiation, EMR

Based on the principle of "capacitance equivalence", the simplified CM current path and its connected cable can be equivalent to EMR (Figure 4). The parasitic capacitance of EMR and PCS is extracted by finite element method (FEM), and then geometric parameter of EMR is obtained by iterative design. The EMR is fed by signal generator to simulate radiation emission of PCS. Furthermore, PCS and EMR are tested in the anechoic chamber, and the radiation emission of two models is in good agreement that verifies the feasibility of the method.

In Figure 4, C_E represents the distributed capacitance between emitting region and PCB ground; C_G represents the distributed capacitance between cables and ground. Let

$$C_E=C_{CM} \quad (1)$$

$$C_G=C_1+C_2 \quad (2)$$

Then the PCS can be replaced by EMR in radiation characteristics. Further, the prediction of far-field electromagnetic radiation in PCS can be conducted by making analysis or experiment on EMR.

The optimal Design of Capacitive Parameter in EMR

Figure 5 shows the process of iterative optimization design on structural parameters of EMR.

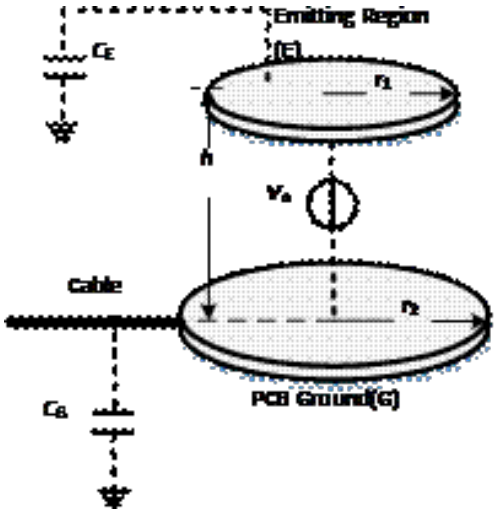

Figure 4: Equivalent prediction model of radiation (EMR)

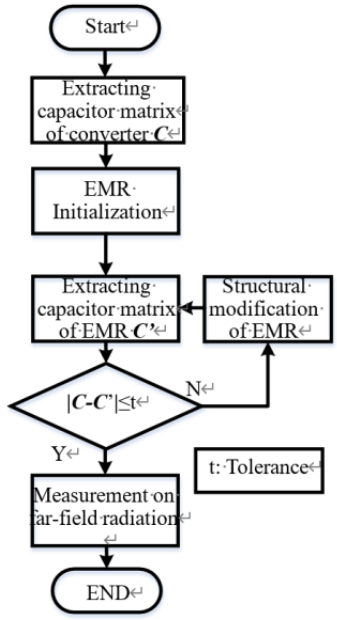

Figure 5: The optimization process of EMR based on capacitances equivalence

The converter model (Table 1) is established in ANSYS, and the capacitance parameter matrix extracted from PCS is

$$\boldsymbol{C}=\begin{bmatrix} C_{11} & C_{12} \\ C_{21} & C_{22} \end{bmatrix}=\begin{bmatrix} 0.128 & 9.226 \\ 9.226 & 3.411 \end{bmatrix}(\text{pF}) \qquad (3)$$

In fact, the matrix is the EMR optimization objective matrix; In equation(3), C_{11} represents the capacitance of C_1, C_{12} and C_{21} represent the capacitance of C_{CM}, C_{22} represents the capacitance of C_2; correspondingly, the matrix in the EMR iterative design process is

$$\boldsymbol{C'}=\begin{bmatrix} C'_{11} & C'_{12} \\ C'_{21} & C'_{22} \end{bmatrix} \qquad (4)$$

Table 1: The structure size of converter/mm

	Length	Width	Height
PCB	43.18	53.56	1.50
Chassis	100.0	100.0	50.00

Based on the previously determined structural dimensions, the structural parameters to be optimized for EMR are only three, that radius r_1 of E, radius r_2 of G, and distance H_{1s} from E to the upper part of the chassis. In order to achieve the convergence quickly, select the initial value of the above parameters according to formula (5) - (7)

$$r_1^{(0)}=\sqrt{\frac{C_{12}h}{\varepsilon\delta}} \qquad (5)$$

$$r_2^{(0)}=\sqrt{\frac{C_{22}h_{2s}}{\varepsilon\delta}} \qquad (6)$$

$$h_{1S}^{(0)}=5h \qquad (7)$$

Let the tolerance t = 10^{-3}. After conducting 10 iterations, the structural parameters of EMR are shown in Table 2. Using the approximate relation to construct the iterative scheme, the times of iterations is effectively reduced, and the result converges to the target value quickly.

Table 2: The structure size of EMR by iteration/mm

	r_1	r_2	h_{1s}
Before	11.26	26.95	3.96
After	5.30	35.01	8.74

Electromagnetic radiation prediction

The Principle of Magnetic Ring Restraining Noise

Electromagnetic radiation can be passively suppressed, such as shielding. Also, there is a more effective method to suppress the noise current actively, such as adding magnetic ring (Figure 6). The magnetic ring not only stores part of noise energy, but also consumes some of it. The common material of magnetic ring is Mn-Zn ferrite and Ni-Zn ferrite. Mn-Zn ferrite has high initial permeability, but it decreases sharply with the increase of frequency after 100kHz. Therefore, in the radiation frequency range of (30-300) MHz, Ni-Zn ferrite magnetic ring with low initial permeability has better high frequency performance is selected.

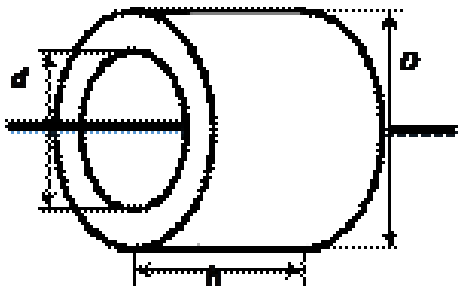

Figure 6: Ferrite ring round transmission line

When the cable passes through the magnetic ring, the equivalent inductance of the magnetic ring is

$$L = \frac{\mu h}{2\pi} \ln \frac{D}{d} \quad (8)$$

Where

$$\mu = \mu' - j\mu'' \quad (9)$$

Correspondingly, the equivalent impedance of the magnetic ring is

$$Z = j\omega L = R_d + j\omega L_d \quad (10)$$

$$R_d = \frac{\mu'' h}{2\pi} \ln \frac{D}{d} \quad (11)$$

$$L_d = \frac{\mu' h}{2\pi} \ln \frac{D}{d} \quad (12)$$

Where R_d can suppress the noise current in the cable; L_d can store the noise current.

Therefore, the magnetic ring can be seen as the series connection of resistance R_d and inductance L_d. If the influence of parasitic capacitance C_d is considered, the magnetic ring can be equivalent to that shown in Fig. 7. In this paper, only a single cable passes through the magnetic ring, and the effect of its capacitance is negligible in the range lower than the resonance frequency. Therefore, the resistance R_d and the inductance L_d are the key parameters to suppress the radiation interference, and their values determine the effect on radiation suppression.

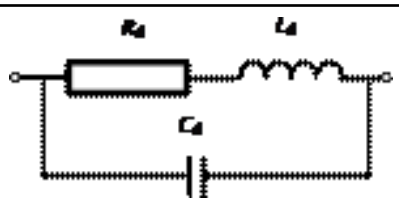

Figure 7: Model with three parameters of ferrite ring

Experiment

In this paper, a boost converter is used as an example. The (30-300) MHz far-field radiation characteristics of boost converter are measured in a 3M anechoic chamber (Fig8). According to the requirements of GJB151A / 152A re102 test standard, the biconical antenna is used to measure the frequency range of (30-200) MHz; the double ridged horn antenna is used to measure the frequency range of (200-300) MHz. The tested boost converter is placed on a 90cm high grounding platform, the largest transmitting surface is facing the test antenna, and the electric field intensity in the vertical polarization direction is tested.

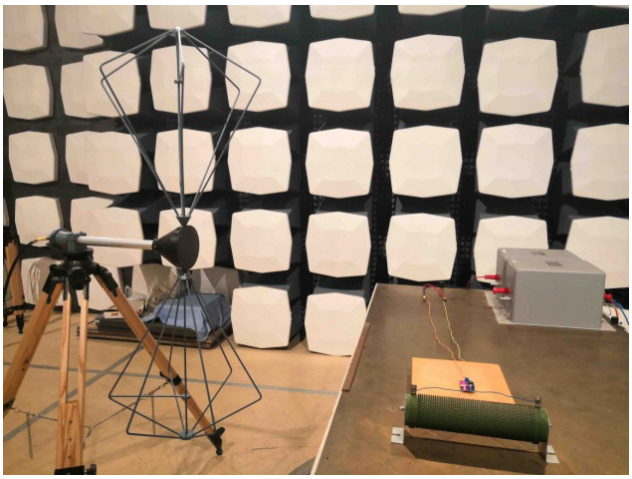

Figure 8: Layout of radiation test in 3m anechoic chamber

The experimental test configuration is shown in Table 3. Data is collected by EMI receiver. The test results are shown in Figure.11.

Table 3: Experimental test configuration

Input/Output voltage/V	8.0/9.0
Length of cables/m	1、0.8、0.6
PCB Length×Width/cm	6.5×3.5
Height/cm	5.0

The experimental layout of EMR radiation prediction is shown in Figure 9. According to the iterative EMR structure parameters, the EMR physical design is carried out. The noise source V_N of boost converter is tested with RIGOL-DS4032 oscilloscope, and the measured V_N waveform is shown in Figure 10. In the 3M anechoic chamber, rigol-dg5351 signal generator is used to simulate the noise source voltage and feed EMR.

The predicted EMR curve is compared with the far-field radiation curve of boost in Figure 11.

Figure 9: Prediction experiment of EMR radiation

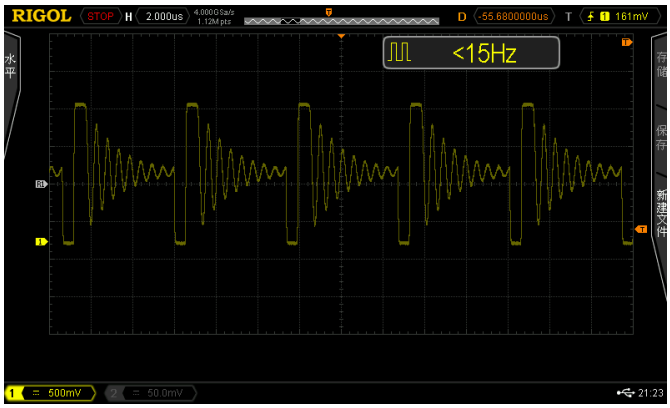

Figure 10: Origin noise

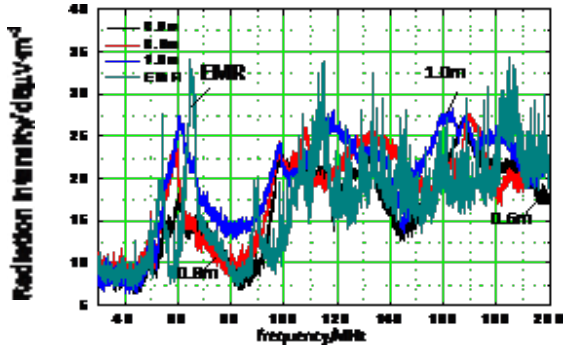

(a) (30-200) MHz (b) (200-300) MHz

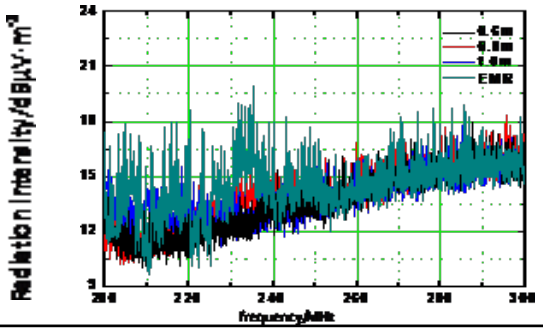

Figure 11: Comparison of radiation EMI after improvement

The results of boost converter and EMR radiation intensity are as shown in Figure 17, the peak value of some frequency points of EMR curve at (30-200) MHz, but the overall trend is basically consistent with the boost converter radiation curve; The variation trend of the radiation intensity within (200-300) MHz and the predicted curve is basically the same as that of the boost converter, which proves the validity of the equivalent method of the capacitive parameters, and also provides a simple method to predict the radiation intensity of the power converter.

Suppression on Radiation Noise

According to the characteristics of the ferrite magnetic ring, the change degree of the scattering matrix is different when the ferrite magnetic ring of different specifications is connected to the input cable, and the ferrite magnetic ring (Table 4) is connected at the place 0.1M away from the input port on the input cable of the converter for testing.

Table 4: Magnetic ring specifications

No.	Size(outer diameter×length×inner diameter)/mm
1	25×14×10
2	33×20×13
3	36×23×13
4	39×27×13

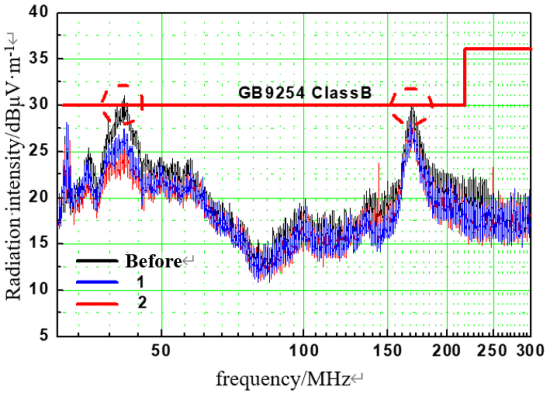

(a) Suppressive effect of No.1 and No.2

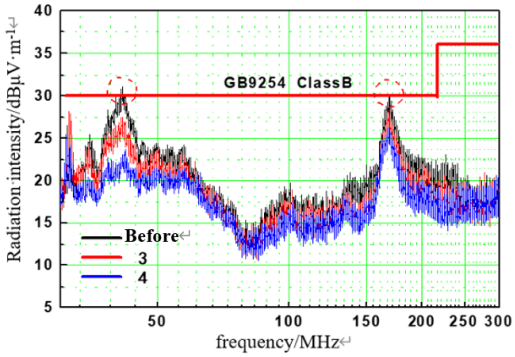

(b) Suppressive effect of No.3 and No.4

Figure 12: Suppression effect of magnetic ring type

Figure 12 shows that magnetic ring during (30-300) MHz range has good suppression effect on the over standard frequency points, and the radiation noise is significantly reduced. The frequency bands meet the GB9254 class B standard and have certain safety margin. Further, the research on noise peak attenuation and magnetic ring specification is shown in Table 5. The attenuation of radiation intensity of No.1-4 magnetic ring increases from 3.6 to 7.8dBμV·m^{-1} at 41.7MHz, and the attenuation increases from 2.3 to 4.8dBμV·m^{-1} at 168.8MHz. It can be seen that the radiation attenuation is positively related to the outer diameter and length of the magnetic ring. Properly increasing the length and outer diameter of the magnetic ring can increase the effect on radiation inhibition.

Table 5: Peak attenuation of radiation frequency point

Number / Radiation intensity	1	2	3	4
$E_{41.7\text{MHz}}$	27.3	26.3	25.9	23.1
$\Delta E_{41.7\text{MHz}}$	3.6	4.6	5.0	7.8
$E_{168.8\text{MHz}}$	27.8	26.3	26	25.3
$\Delta E_{41.7\text{MHz}}$	2.3	3.8	4.0	4.8

Conclusion

In this paper, the boost converter is taken as the research object. Based on the principle of "capacitance parameter" equivalence, the numerical calculation method is used to study the PCs expansion system, and the following conclusions are obtained:

(1) It is found that the far-field radiation of PCS mainly comes from CM noise current, and the radiation caused by DM current in the far-field area offsets each other, which can be ignored. Therefore, the radiation model is simplified and the equivalent prediction model of radiation (EMR) is obtained.

(2) The "capacitance parameters" of PCS and EMR are extracted by FEM. Based on the principle of "capacitance equivalence", the EMR is designed iteratively. The radiation characteristics of PCS can be predicted by EMR simulation or experiment, which provides a convenient way to study the far-field radiation characteristics of PCS.

(3) Compared with the radiation characteristics of PCs and EMR, the radiation field intensity of PCs and EMR is consistent, which proves the validity and correctness of the method in this paper. Furthermore, we found that installing magnetic ring can reduce the noise current effectively.

References

1. Clayton R Paul. Introduction to electromagnetic compatibility. New York: Wiley, 2005.
2. Clayton R Paul. Analysis of multi-conductor transmission lines 2nd Edition. New York: Wiley, 2013.
3. He JP, Ji KJ, Fu Q, WANG RQ. Common mode far field radiation model & its characteristics of a flyback power supply. Advanced Technology of Electrical Engineering and Energy. 2012;31(3):25-30.
4. Shim HW, Hubing TH. A closed-form expression for estimating radiated emissions from the power planes in a populated printed circuit board. IEEE Transactions on Electromagnetic Compatibility. 2006;48(1):74-81.
5. Shinde S, Masuda K, Shen G, Patnaik A, Makharashvili T, Pommerenke D, et al. Radiated EMI estimation from DC–DC converters with attached cables based on terminal equivalent circuit modeling. IEEE Trans. on Electromagnetic Compatibility. 2017;60(6):1769-1776. DOI: 10.1109/TEMC.2017.2782659
6. Shim HW, Hubing TH. Model for estimating radiated emissions from a printed circuit board with attached cables due to voltage-driven sources. IEEE Trans. on Electromagnetic Compatibility. 2005;47(4):889-907. DOI: 10.1109/TEMC.2005.859060
7. Chen HL, Wang T, Feng L, Chen G. Determining far-field EMI from near-field coupling of a power converter. IEEE Transactions on Power Electronics. 2014;29(10):5257-5264. DOI: 10.1109/TPEL.2013.2291442
8. Laour M, Tahmi R, Vollaire C. Modeling and analysis of conducted and radiated emissions due to common mode current of a buck converter. IEEE Transactions on Electromagnetic Compatibility. 2017;59(4):1260-1267. DOI: 10.1109/TEMC.2017.2651984
9. Wang QD, An Z Y, Zheng YL, et al. Electromagnetic radiation mechanism and noise suppression method for hybrid electric bus. Transactions of China Electrotechnical Society. 2014;29(9):225-331.
10. Gan ZY, Wang YH, Zhang JG, et al. Suppression of HF passive interference in transmission lines by using magnetic tube. High Voltage Engineering. 2017;43(5): 1722-1728.
11. Qiu RQ, Zhu F, Gao CX. Suppressing effect of ferrite magnetic rings on induced current of field-to-line coupling. High Voltage Engineering. 2018;44(9): 2732-2737.
12. Guan YG, Guo PQ, Chen WJ, et al. Test study on suppressing VFTO in 252 kV GIS by ferrite magnetic rings. High Voltage Engineering. 2014;40(7):1977-1985.
13. Zhang H, Zhao ZB, Liu L. Test research on the suppressing radio interference of DC transmission lines by ferrite cores. Transactions of China Electro technical Society. 2013;28(S2):180-184.